

Growth and characterization of InAs/GaSb photoconductors for long wavelength infrared range

H. Mohseni, E. Michel, Jan Sandoen, and M. Razeghi

Electrical and Computer Engineering Department, Center for Quantum Devices, Northwestern University, Evanston, Illinois 60208

W. Mitchel and G. Brown

Wright Laboratory, Materials Directorate, WPAFB, Ohio 45433-7707

(Received 29 May 1997; accepted for publication 8 July 1997)

In this letter we report the molecular beam epitaxial growth and characterization of InAs/GaSb superlattices grown on semi-insulating GaAs substrates for long wavelength infrared detectors. Photoconductive detectors fabricated from the superlattices showed photoresponse up to 12 μm and peak responsivity of 5.5 V/W with Johnson noise limited detectivity of $1.33 \times 10^9 \text{ cm Hz}^{1/2}/\text{W}$ at 10.3 μm at 78 K. © 1997 American Institute of Physics. [S0003-6951(97)03236-1]

Infrared imaging in the 8–12 μm wavelength has many medical, industrial, and military applications. After two decades of progress, the currently dominant HgCdTe technology¹ still cannot provide detectors with high sensitivity, resolution, and room-temperature operation. The major drawbacks of HgCdTe detectors are the difficulty in growth, nonuniformity due to high sensitivity to the composition, large tunneling currents, and high Auger recombination rate.² An alternative structure in the 8–12 μm range is quantum well infrared photodetector (QWIP).³ However, high thermal generation rate and short carrier lifetime limits high-temperature operation and quantum efficiency of QWIPs.⁴ As another alternative for infrared photodetectors, type II superlattices have been studied.^{5–7} The II–VI, HgTe/CdTe and the III–V, InAs/Ga_xIn_{1–x}Sb type II superlattices have shown promising results comparable to HgCdTe photoconductors at long wavelengths.^{6,7} However, it was found that the growth and processing of these II–VI materials are more difficult than III–V compounds.

Lower dark current and higher operating temperature is expected for InAs/Ga_xIn_{1–x}Sb superlattices in comparison to HgCdTe, because of the higher effective mass of electrons and holes and slower Auger recombination.^{8,9} In this letter, we present the results of photoconductive detectors fabricated from InAs/GaSb superlattices.

The superlattices were grown by molecular beam epitaxy on semi-insulating GaAs substrates. A 4 μm GaSb buffer layer was grown directly on 3 in. GaAs substrates. The wafer was then broken into $\sim 1 \text{ cm}^2$ pieces and indium mounted to molybdenum blocks. Uncracked elemental Ga, In, As, and Sb were used as source materials. InAs is found to have a very narrow window for planar growth, while high quality GaSb can be grown in a wider range of growth conditions. The optimum growth conditions for InAs layers were found to be $T=400^\circ\text{C}$ according to a pyrometer, V to III incorporation rate ratio ≈ 3 , and a growth rate of 0.5 monolayer/s. In this condition, reflection high energy electron diffraction showed 2×4 reconstruction patterns. The structure consisted of a superlattice with 48 Å InAs, 48 Å GaSb, one monolayer of InSb at the interfaces, and a thin 200 Å GaSb cap layer.

The quality of the superlattices was assessed by struc-

tural, electrical, and optical characterization. A high resolution x-ray diffractometer was used to investigate the structure of the material. X-ray diffraction simulation has also been performed to verify the superlattice structures. Figure 1 shows good agreement between the x-ray diffraction spectra of the two 50-period superlattices and the simulated spectra. It also indicates excellent reproducibility and smooth interfaces.

Since electrons and holes are confined in InAs and GaSb, respectively, we could not use the Hall measurement technique on superlattices because of the high sheet density of electrons and holes in InAs and GaSb layers. The overall Hall coefficient for this material, with two dominant channels of electrons and holes can be approximated as¹⁰

$$R_H = \frac{\frac{\mu_p \sigma_p}{1 + \mu_p^2 B^2} - \frac{\mu_n \sigma_n}{1 + \mu_n^2 B^2}}{\left(\frac{\sigma_p}{1 + \mu_p^2 B^2} + \frac{\sigma_n}{1 + \mu_n^2 B^2} \right)^2 + B^2 \left(\frac{\mu_p \sigma_p}{1 + \mu_p^2 B^2} - \frac{\mu_n \sigma_n}{1 + \mu_n^2 B^2} \right)^2}, \quad (1)$$

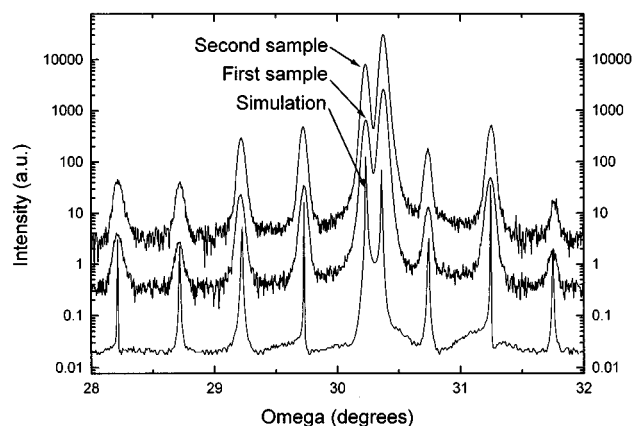


FIG. 1. High resolution x-ray diffraction of two samples and the simulation result. Although one of the samples was grown one week after the other, they are almost identical and the simulation is also in good agreement with them.

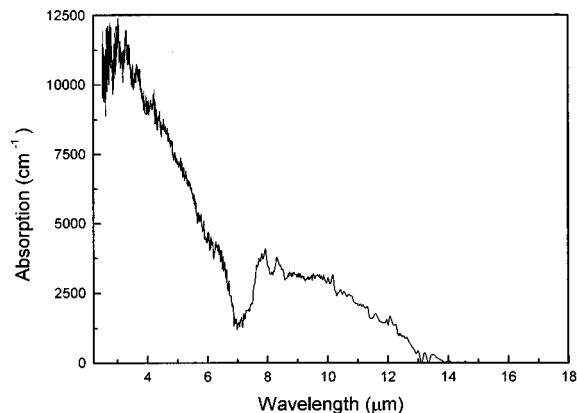


FIG. 2. Room-temperature absorption spectra of a 0.5 μm InAs/GaSb superlattice.

where B is the magnetic field in the Hall measurement, and σ and μ are the conductivity of each channel and the mobility of carriers. The formula shows clearly that the overall Hall mobility can be much smaller than the real mobility of electrons or holes if the numerator approaches zero. As the transport of electrons is more important for photodetector operation due to its higher mobility, a single quantum well of InAs was grown to examine this property. This provided a simple, fast method for electrical assessment of the interface quality. After the optimization of growth conditions, in-plane room-temperature mobility of electrons in a 75 Å InAs well increased from 5000 to 14 000 $\text{cm}^2/\text{V s}$ which is about half the value of bulk InAs.

A Galaxy 3000 Fourier transform infrared (FTIR) spectrometer was used to obtain the optical characteristics of the superlattices. Figure 2 shows the room-temperature optical absorption spectra of the superlattice. The effect of the substrate and GaSb buffer layer was removed by measuring the background with a substrate and GaSb buffer layer. Fabry–Perot oscillations were reduced by positioning the samples at Brewster’s angle to the direction of incident light. The absorption edge at $\sim 14 \mu\text{m}$ is in good agreement with the theoretical 14.4 μm absorption edge at room temperature. The theoretical cutoff wavelength has been calculated using an envelope function approximation containing the strain effect.¹¹ The calculated energy levels are at the Γ point which is a good approximation since the applied electrical field is about tens of volts per centimeter. We used the calculated values of energy band within Van de Walles¹² model for InAs and GaSb.

The photoconductor devices were prepared by making Ohmic contacts either with indium annealing or aluminum deposition and etching. The samples were then mounted to a copper heatsink and attached to the cold finger of a liquid nitrogen cryostat equipped with a temperature controller. Spectral photoresponse was measured with the same FTIR spectrometer system used for the absorption measurement. The samples were illuminated through the front side at normal incidence. Absolute spectral response of the photodetectors was calculated using the relative spectral response and calibrated blackbody measurement data. The responsivity before correction can be calculated as

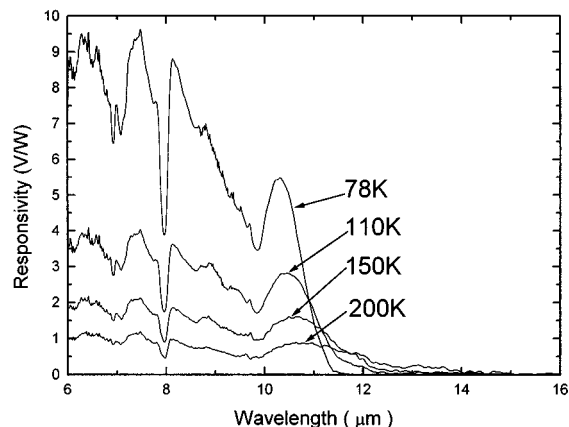


FIG. 3. Responsivity of the photoconductor at 8–12 μm range.

$$R_v^* = \frac{V_p}{\frac{(D_A^2 A_d)}{4r^2} \sigma T_{BB}^4}, \quad (2)$$

where V_p is the measured voltage of the detector after canceling the effect of the chopper and absorption of the cryostat window, D_A is the blackbody aperture diameter, and r is the distance between the aperture and the detector. A_d is the area of the sample, σ is the Stefan–Boltzmann constant, and T_{BB} is the temperature of the blackbody. To determine absolute responsivity R_v , the overlap of the relative spectral responsivity of the detector $S(\lambda)$, and the blackbody spectra, $M(T_{BB}, \lambda)$ was used as the scale factor:

$$R_v = k R_v^*; k = \frac{\sigma T_{BB}^4}{\int_0^\infty M(T_{BB}, \lambda) S(\lambda) d\lambda}. \quad (3)$$

Figure 3 shows the responsivity of a sample at various temperatures. Although most of the spectra can be explained with possible interband transitions, the exact mechanisms of the feature at 8 μm have yet to be determined. The measurement shows a peak responsivity of 5.5 V/W at 10.3 μm at 78 K. To the best of our knowledge, this is the highest responsivity reported on photodetectors fabricated from InAs/GaSb superlattices. The Johnson noise limited detectivity¹³ was $1.33 \times 10^9 \text{ cm Hz}^{1/2}/\text{W}$ at 10.3 μm and 78 K. This value is comparable to $2.5 \times 10^9 \text{ cm Hz}^{1/2}/\text{W}$, the best reported Johnson noise limited detectivity of InAs/Ga_xIn_{1-x}Sb superlattices at the same wavelength and temperature.¹⁴ Although the incorporation of In in GaSb should improve the absorption theoretically, it seems that the superior quality of binary compositions compared to the ternary is also an important factor. Also, the sensitivity of the cutoff wavelength of InAs/Ga_xIn_{1-x}Sb superlattices to the value of x , especially at longer wavelengths, is very high.¹⁵ Therefore, uniformity and reproducibility of the InAs/Ga_xIn_{1-x}Sb superlattices are lower than the InAs/GaSb superlattices.

The authors would like to thank Y. S. Park, M. Yoder, and C. Wood of Office of Naval Research, R. Balcerak and L. N. Durvasula of DARPA, A. Husain and H. O. Everitt of Army Research Office, M. Prairie, and G. Witt of the Air Force for their continued support and encouragement.

- ¹A. Rogalski, *Opt. Eng. (Bellingham)* **33**, 1392 (1994).
- ²A. Reine, A. K. Sood, and T. J. Tredwell, *Semicond. Semimet.* **18**, 201 (1981).
- ³C. Jelen, S. Slivken, J. Hoff, G. J. Brown, and M. Razeghi, *Appl. Phys. Lett.* **70**, 360 (1997).
- ⁴M. A. Kinch and A. Yariv, *Appl. Phys. Lett.* **55**, 2093 (1989).
- ⁵G. A. Sai-Halasz, R. Tsu, and L. Esaki, *Appl. Phys. Lett.* **30**, 651 (1977).
- ⁶D. L. Smith, T. C. McGill, and J. N. Schulman, *Appl. Phys. Lett.* **43**, 180 (1983).
- ⁷C. Mailhiot and D. L. Smith, *J. Vac. Sci. Technol. A* **7**, 445 (1989).
- ⁸E. R. Youngdale, J. R. Meyer, C. A. Hoffman, F. J. Bartoli, C. H. Grein, P. M. Young, H. Ehrenreich, R. H. Miles, and D. H. Chow, *Appl. Phys. Lett.* **64**, 3160 (1994).
- ⁹C. H. Grein, P. M. Young, H. Ehrenreich, and T. C. McGill, *J. Electron. Mater.* **22**, 1093 (1993).
- ¹⁰E. V. Kutchis, *Galvanomagnetic Effects and Methods of Their Investigations* (Izd. Radiosvyaz, Moscow, 1990).
- ¹¹J. Y. Marzin, *Heterostructures and Semiconductor Superlattices*, edited by G. Allan (Springer Verlag, Berlin, 1985), p. 161.
- ¹²C. G. Van de Walle, *Phys. Rev. B* **39**, 1871 (1989).
- ¹³A. Rogalski, *Infrared Photon Detectors* (SPIE, Bellingham, WA, 1995), p. 15.
- ¹⁴J. L. Johnson, L. A. Samoska, A. C. Gossard, J. Merz, M. D. Jack, G. R. Chapman, B. A. Baumgratz, K. Kosai, and S. M. Johnson, *J. Appl. Phys.* **80**, 1116 (1996).
- ¹⁵J. H. Rosland and T. G. Andersson, *Superlattices Microstruct.* **16**, 77 (1994).